



Chemical states of gold doped in ZnO films and its effect on electrical and optical properties



Y. Xu ^{a,b}, B. Yao ^{a,b,*}, Y.F. Li ^a, Z.H. Ding ^a, J.C. Li ^a, H.Z. Wang ^a, Z.Z. Zhang ^c, L.G. Zhang ^c, H.F. Zhao ^c, D.Z. Shen ^c

^a State Key Lab of Superhard Materials and Department of Physics, Jilin University, Changchun 130023, People's Republic of China

^b Key Laboratory of Physics and Technology for Advanced Batteries, Ministry of Education and Department of Physics, Jilin University, Changchun 130023, People's Republic of China

^c Laboratory of Excited State Processes, Changchun Institute of Optics, Fine Mechanics and Physics, Chinese Academy of Sciences, Changchun 130021, People's Republic of China

ARTICLE INFO

Article history:

Received 3 June 2013

Received in revised form 27 September 2013

Accepted 29 September 2013

Available online 10 October 2013

Keywords:

ZnO film
Magnetron sputtering
Chemical state
Au doping

ABSTRACT

Gold-doped ZnO (ZnO:Au) films were grown on quartz substrates at room temperature by radio frequency magnetron sputtering technique and then annealed in the temperature ranging from 350 to 800 °C in argon ambience. It is found that the Au substitute for Zn in positive univalence ($\text{Au}_{\text{Zn}}^{1+}$) in the as-grown ZnO:Au film. When the ZnO:Au is annealed above 600 °C, some of the $\text{Au}_{\text{Zn}}^{1+}$ begin to precipitate from the ZnO:Au and become metal Au existing in the grain boundaries of the ZnO:Au, implying that the solid solubility of Au in ZnO decreases with increasing temperature. p-type conductivity is obtained in the ZnO:Au annealed at 350 °C, but the conductivity changes gradually from p-type to n-type with increasing annealing temperature. The optical band-gap of the ZnO:Au shows red-shift compared to undoped ZnO. The ZnO:Au shows room temperature photoluminescence (PL) quenching as annealed below 800 °C, but has two weak PL peaks, located at 2.417 and 3.299 eV, respectively, as annealed at 800 °C. The electrical and optical properties of the ZnO:Au are affected by the chemical states and content of the Au doped, and the mechanism of the effects are suggested in the present paper.

© 2013 Elsevier B.V. All rights reserved.

1. Introduction

In recent years, wide bandgap semiconductors involving SnO_2 , TiO_2 , ZnO, AlN, etc. have been extensively studied as they have numerous potential applications in many fields, such as gas sensors, transparent conducting thin films, and catalysis [1–7]. Such semiconductors with interesting and useful properties are attracting more and more research attention. Among these semiconductors, considering the potential applications in laser diodes (LDS) and short-wavelength semiconductor light-emitting diodes (LEDs) [8,9], ZnO has been most widely researched due to its direct wide band gap of 3.37 eV and larger exciton binding energy of 60 meV at room temperature [10–12]. However, the greatest problem that hinder the application and development of ZnO based optoelectronic device remains to be the fabrication of reliable and stable p-type ZnO thin films [13,14]. To overcome these difficulties, a great deal of effort has been devoted to fabricate p-type ZnO by doping of various elements, such as group-I (Li [15], Na [16] and K [17]) and group-V (N [18], P [19], As [20] and Sb [21]) elements

in the recent years, but due to the low dopant solubility, self-compensation of shallow acceptors from native donor defects and doping donor defects (such as Li_i [22], and $(\text{N}_2)_\text{O}$ [23]) as well as the poor crystal quality, the optimal choice of acceptor species remains to be determined, the key question on the p type conductivity of ZnO is still open.

First-principle calculation predicted that the formation energies of group-IB (Cu, Ag and Au) ions with positive univalence at Zn sites of ZnO are much lower than those at the interstitial sites, hence substitutional doping of IB-group element in ZnO can greatly avoid the self-compensation, and is considered as an effective p-type doping method [24]. However, since IB-group elements have three kinds of valence and only univalent IB-group ion occupying Zn site of ZnO acts as acceptor, realization of substitutional doping and controlling of the chemical states are very important for obtaining p-type IB-group element doped ZnO. Up to now, Cu-doped ZnO and Ag-doped ZnO have been synthesized and investigated by several groups. He et al. [25] has obtained Cu-doped ZnO nanorod arrays, where Cu exist in the chemical states of Cu^{1+} and Cu^{2+} in the ZnO, and Cu^{1+} can convert into Cu^{2+} by annealing. In our previous study [26] p-type ZnO films has been synthesized by alloying of S with ZnO and heavy doping of Cu with magnetron sputtering, where some of Cu exist in the state of $\text{Cu}_{\text{Zn}}^{1+}$. Lee et al. [27] has obtained Ag-doped ZnO films by pulsed

* Corresponding author at: State Key Lab of Superhard Materials and Department of Physics, Jilin University, Changchun 130023, People's Republic of China. Tel.: +86 13159640416; fax: +86 431 86171688.

E-mail address: binyao@jlu.edu.cn (B. Yao).

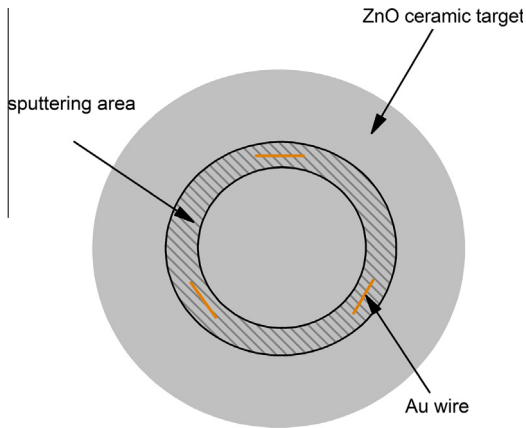


Fig. 1. Schematic diagram of the ceramic target used for fabrication of the ZnO:Au film by radio frequency magnetic sputtering.

laser deposition, where some of Ag substitute for Zn in univalence ($\text{Ag}_{\text{Zn}}^{1+}$) and some of Ag exist in the grain boundaries or surface in the chemical state of metal (Ag^0). However, literatures about Au-doped ZnO (ZnO:Au) are reported little up to now, the chemical states of Au doped in ZnO, as well as their effect on electrical and optical properties are still under investigation. Key question on the chemical states of Au in the ZnO:Au is still open.

In the present work, in order to explore the possibility of preparation of p-type ZnO with good luminescence by Au doping, the ZnO:Au films were deposited on quartz substrates by magnetron sputtering and post annealing techniques, chemical states of the Au doped in the ZnO film was characterized and the effect of chemical states of the Au on electrical and optical properties of the ZnO:Au was investigated.

2. Experimental details

JGP450 magnetron sputtering apparatus (made in Chinese academy of science Shenyang scientific instrument factory, China) was used for sputtering deposition. Undoped ZnO films were grown on quartz substrates at room temperature by magnetron sputtering of the ZnO (99.99%) ceramic target, while Au-doped ZnO films were prepared by sputtering of the ZnO ceramic target with Au (99.999%) wires on its surface, as schematically shown in Fig. 1, and the Au doping content is controlled by adjusting the ratio of surface area of the Au wires to the sputtering area. High purity argon was used as working gas, which was introduced into the growth chamber when the chamber was evacuated to a base pressure of 6×10^{-4} Pa, and the working pressure was kept at 1 Pa during depositing process. All the as-grown films were cut into 5 mm square small pieces and annealed at 350, 600 and 800 °C, respectively, under argon atmosphere for 15 min, the film thickness was estimated to be 900 nm by the cross section morphology scanning electron microscopy (SEM) image of the film.

Structures of the films were characterized using Rigaku D/Max-RA X-ray diffractometer (XRD) with Cu K α radiation ($\lambda = 1.5418 \text{ \AA}$). The chemical state of Au in the ZnO:Au was detected by X-ray photoelectron spectroscopy (XPS) (ESCALAB 250 XPS instrument) with Al K α ($h\nu = 1486.6 \text{ eV}$) X-ray radiation source, prior to measurements all the films were etched by Ar^+ ions for 120 s, and all XPS spectra were calibrated by C1s peak (284.6 eV). Surface morphology of the films was detected by field emission scanning electron microscopy (FE-SEM). The electrical properties were measured with the van der Pauw configuration by a Hall Effect measurement system (Lakeshore HMS 7707) at room temperature with magnetic field scope from 3 to 15 KG, and ohmic contacts of the electrodes were confirmed initially. Optical band gap of the films were characterized using an UV-Vis spectrophotometer (Shimadzu, Kyoto, Japan (UV-3101PC)). The room temperature photoluminescence (PL) spectra of the ZnO:Au were recorded by the UV Labran Infinity Spectrophotometer, which was excited by the 325 nm line of a He–Cd laser with a power of 50 mW.

3. Result and discussion

The structures of the as-grown and annealed undoped ZnO (denoted as ZnO) and ZnO:Au films are analyzed via XRD, as shown in Fig. 2. For the as-grown and 350, 600 and 800 °C-annealed ZnO films, only (002) diffraction peaks are observed, as shown in Fig. 2(a–d), indicating all the films are c-axis preferred orientation.

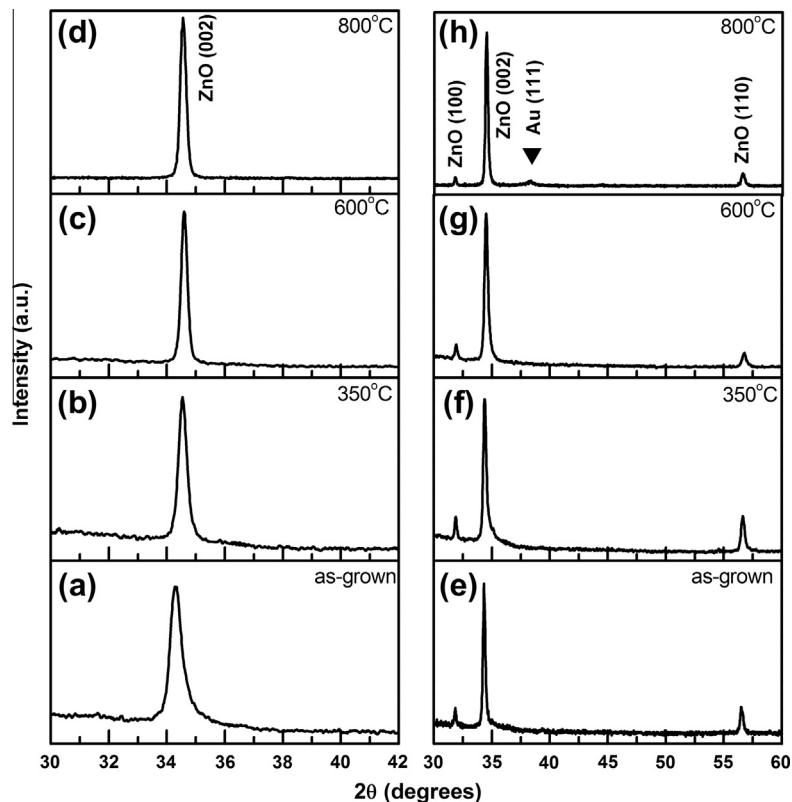


Fig. 2. XRD patterns of the as-grown and different temperature annealed (a)–(d) undoped ZnO and (e)–(h) ZnO:Au films.

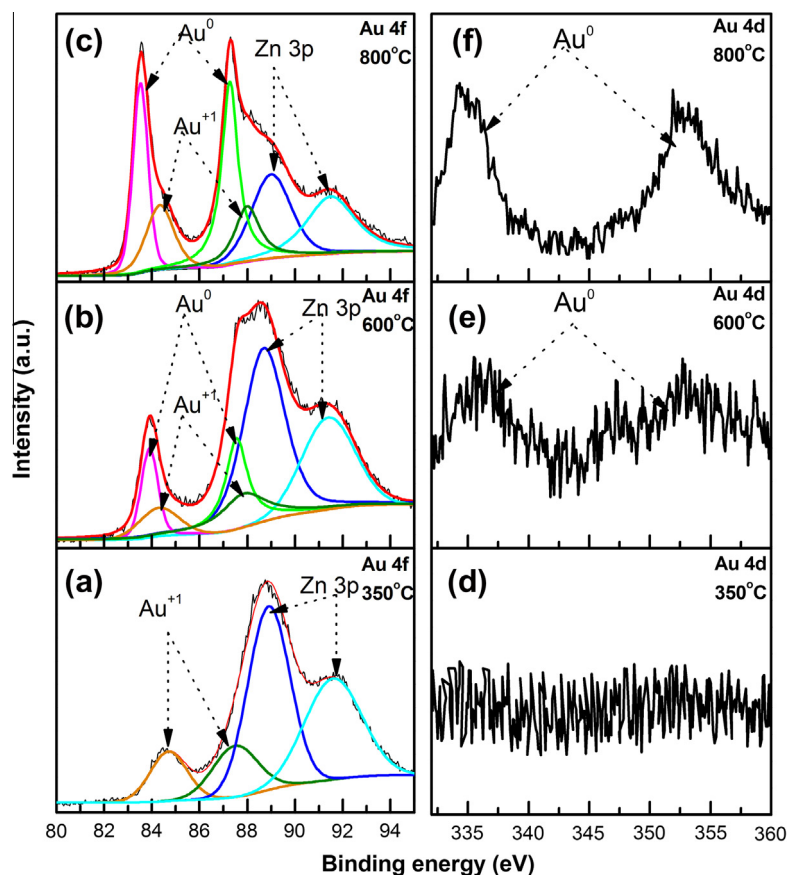


Fig. 3. XPS spectra of (a)–(c) the Au 4f of the different temperature annealed ZnO:Au films and XPS spectra of (d)–(f) the Au 4d of the ZnO:Au films annealed at different temperature.

For the as-grown and 350, 600 °C-annealed ZnO:Au films, diffraction peaks with diffraction angles closed to that of (100), (002) and (110) peak of ZnO with wurtzite structure (PDF No. 36–1451) are observed, and no diffraction peak of metal Au or Au related phase is detected, as shown in Fig. 2(e–g). However, as the annealing temperature reaches 800 °C, Au (111) peak located at 38.23° is detected (PDF No. 04–0784) in the 800 °C-annealed ZnO:Au besides the (100), (002) and (110) diffraction peaks, as shown in Fig. 2(h), implying that some of Au incorporate into ZnO to form the ZnO:Au in the deposition process but some of the Au in the ZnO:Au precipitate as the ZnO:Au is annealed.

It is well known that Au has three kinds of chemical states including metal Au, Au^{1+} and Au^{3+} . In order to well understand the chemical states of Au in the ZnO:Au films. XPS measurement was performed for the annealed ZnO:Au films. The Au 4f XPS spectra for the 350, 600 and 800 °C-annealed ZnO:Au are illustrated in Fig. 3(a–c). Since the XPS spectra of Zn 3p and Au 4f overlaps at the binding energy interval of 80–96 eV [28], the measured XPS spectrum was fitted using Lorentz-Gaussian fitting method. For the 350 °C-annealed ZnO:Au, the XPS spectrum can be fitted into four peaks, located near the binding energy of 84.4, 87.2, 88.6 and 91.3 eV, respectively, which correspond to $\text{Au}^{1+} 4f_{7/2}$, $\text{Au}^{1+} 4f_{5/2}$, $\text{Zn}^{2+} 3p_{3/2}$ and $\text{Zn}^{2+} 3p_{1/2}$, respectively, suggesting that the Au exist in the univalence state and substitute for Zn in the as-grown and 350 °C-annealed ZnO:Au [29–31]. For the 600 and 800 °C-annealed ZnO:Au, the XPS spectra of Au 4f are fitted into six peaks, as shown in Fig. 3(b) and (c), the two additional peaks located near 83.5 and 87.5 eV are observed besides the peaks of the Au^{1+} and Zn^{2+} [29], which are attributed to $\text{Au}^0 4f_{7/2}$ and $\text{Au}^0 4f_{5/2}$, respectively. With increasing annealing temperature, the intensity of $\text{Au}^0 4f$ peak

Table 1

The relative content of Au, Zn and O in the ZnO:Au films measured by XPS.

Sample	Annealing temp. (°C)	Zn content (at.%)	O content (at.%)	Au^0 content (at.%)	Au^{1+} content (at.%)
ZnO:Au	350	52.4	44.1	–	3.5
ZnO:Au	600	48.7	48.1	1.5	1.7
ZnO:Au	800	57.6	37.8	3.1	1.5

increases evidently, meanwhile, the intensity of $\text{Au}^{1+} 4f$ decreases, indicating that some of Au^{1+} precipitate from ZnO:Au and form metal Au as the annealing temperature is above 600 °C. This result is further confirmed by the Au 4d XPS spectra of the 350, 600 and 800 °C-annealed ZnO:Au, as shown in Fig. 3(d–f). Peaks located near 335.3 and 353.5 eV, corresponding to $\text{Au}^0 4d_{3/2}$ and $\text{Au}^0 4d_{5/2}$ are detected only in the ZnO:Au films annealed at 600 and 800 °C, moreover, the intensity of the peaks increases with the increase of annealing temperature, indicating the content of metal Au increases with the increasing annealing temperature.

Table 1 gives the content of Au^0 , Au^{1+} , Zn and O of the 350, 600 and 800 °C-annealed ZnO:Au estimated using XPS data of Fig. 3 and following formula:

$$C_x = \frac{I_x/S_x}{\sum_i I_i/S_i} \quad (1)$$

where I_x and S_x are the peak area and sensitivity factor of the selected element, respectively, and I_i and S_i are the peak area and sensitivity factor for the zinc, oxygen and gold, respectively. It can be

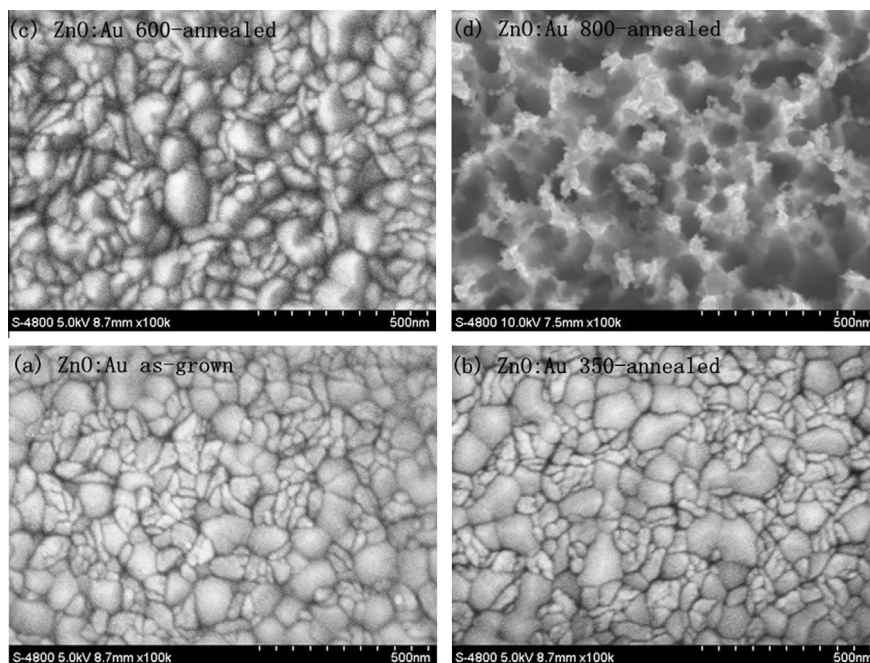


Fig. 4. Surface morphology SEM images of the (a) as-grown, (b) 350 °C, (c) 600 °C, and (d) 800 °C-annealed ZnO:Au.

seen from Table 1 that the ZnO:Au is Zn-rich as annealed at temperatures not larger than 600 °C, and the ratio of Zn to O decreases and is closed to the stoichiometric ratio of 1:1 with increasing temperature, due to that more and more Zn escape from ZnO with increasing annealing temperature [32]. However, upon annealing temperature reaches 800 °C, oxygen begin to escape greatly from the film in the rate higher than Zn, leading to the content of Zn is much larger than that of O and the formation of large amount of V_O and Zn_i donors. In addition, it is also found that the Au^{1+} begins to precipitate from the ZnO:Au at annealing temperatures more than 600 °C and becomes metal Au, and the content of metal Au (Au^0) increases while the content of Au^{1+} decreases with the increasing annealing temperature, which meaning that the solid solubility of Au in ZnO decreases with increasing annealing temperature.

In order to investigate the change of composition of the ZnO:Au with temperature and position of the metal Au by analysis of surface morphology of the film, SEM was performed for the ZnO:Au films. It can be seen from Fig. 4(a–c) that the surfaces of the as-grown ZnO:Au film and the films annealed at 350 and 600 °C consist of dense nanoparticles, and the morphology of the surface has not apparent change with the increasing annealing temperature. However, compared to Fig. 4(a–c), the surface occurs obvious change when the ZnO:Au is annealed at 800 °C, and there appears a lot of holes in the surface, as shown in Fig. 4(d). The obvious change confirms that a large amount of O and Zn escape from ZnO at annealing temperature of 800 °C, concluded from XPS measurement. In addition, no Au nanoparticle or cluster is observed on the surfaces, as shown in Fig. 4(a–d). Moreover, XPS measurements for the ZnO:Au annealed at 600 and 800 °C also indicate that the relative content of metal Au is almost the same before and after surface stripping. Therefore, it can be concluded that the metal Au does not exist on the surface but in the grain boundaries of the ZnO:Au.

Hall-effect measurement results of the ZnO and ZnO:Au films annealed at various temperatures are summarized in Table 2. It can be seen that they show different electrical properties with annealing temperature. The insulating properties of the

Table 2

The electrical properties of the ZnO and ZnO:Au films annealed at various temperatures.

Sample	Annealing temp (°C)	Resistivity (Ω cm)	Carrier density (cm^{-3})	Mobility (cm^2/Vs)	Type
ZnO	350	Insulated	–	–	–
ZnO	600	1.72×10^2	1.39×10^{16} 5.29×10^{16}	2.82 0.74	n p
ZnO	800	1.90×10^1	3.33×10^{17}	1.00	n
ZnO:Au	350	1.63×10^4	2.38×10^{15}	0.16	p
ZnO:Au	600	Insulated	–	–	–
ZnO:Au	800	2.40×10^3	7.16×10^{15}	0.37	n

350 °C-annealed ZnO is due to poor crystal quality. The p/n properties means that the 600 °C-annealed ZnO shows arbitrary conduction type at different applied magnetic fields, suggesting that native acceptor defects have been considerably formed and compete with the native donors. As annealing temperature increases from 600 °C to 800 °C, the undoped ZnO return to n-type conduction due to that native donor defects become dominate again. Differing from the ZnO, the ZnO:Au annealed at 350 °C shows p-type conduction, which is due to the high doping content of Au^{1+} acceptor in the films, which compensated most of the native donor defects, as shown in Table 1. When annealing at 600 °C, due to precipitation of Au_{Zn}^{1+} acceptor from the ZnO:Au, the acceptors are mostly compensated by native donors, resulting in insulating properties of the 600 °C-annealed ZnO:Au. When annealed at 800 °C, more Zn_i generate and content of Au^{1+} decreases in the ZnO:Au, so the ZnO:Au conducts in n-type. However, the electron concentration is near two order of magnitude smaller than that of the ZnO annealed at 800 °C, which is due to existence of the Au^{1+} acceptor in the 800 °C-annealed ZnO:Au. The results of Tables 1 and 2 indicate that the Au can incorporate into ZnO in Au^{1+} and occupy the Zn site (denoted as Au_{Zn}^{1+}), and the Au_{Zn}^{1+} acts as acceptor. The evolution of conductivity with increasing annealing

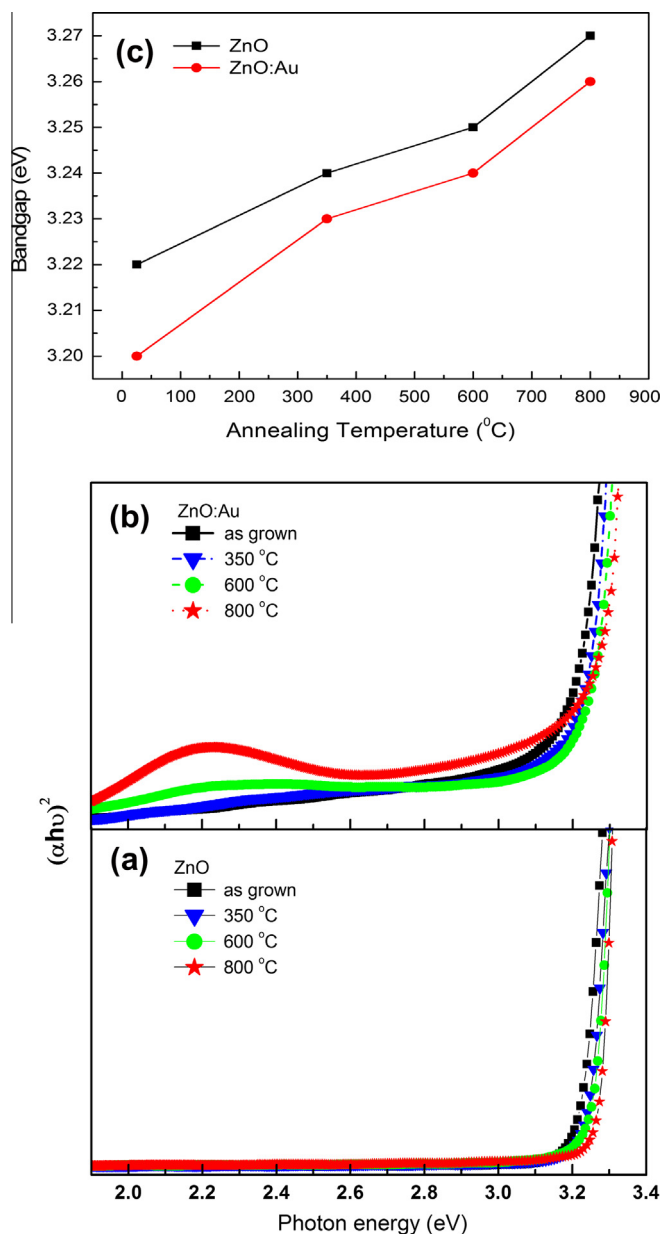


Fig. 5. The plots of $(\alpha h\nu)^2$ vs. photon energy $h\nu$ of the as-deposited and different temperature annealed (a) undoped ZnO, (b) ZnO:Au films. (c) Plots of the band gap of the ZnO and ZnO:Au films as a function of the annealing temperature.

temperature is related to the change of the relative content of the $\text{Au}_{\text{Zn}}^{1+}$ and intrinsic defects.

Fig. 5 shows the plot of $(\alpha h\nu)^2$ vs. the photon energy $h\nu$ of the as-deposited and annealed ZnO and ZnO:Au film. It can be seen from Fig. 5(a) and (b) that the optical band gap gradually shift from 3.220 to 3.269 eV with increasing annealing temperature for the ZnO but from 3.205 to 3.258 eV for the ZnO:Au. The blue-shift of the band gap is due to that both films are subjected to biaxial tensile stress induced by thermal mismatch between the films and substrate [33]. It is worth noting that the band edge of the ZnO:Au is smaller than that of the ZnO at the same preparation conditions, as shown in Fig. 5(c), which is mainly due to the dopant effect of Au. Au, as a group-IB element, its occupied d orbital energies is near the oxygen p level, and both the O p and the Au d orbitals have t_2 symmetry in tetrahedral environment [24]. When the Au atom occupies the Zn site, the strong p-d coupling between Au and O occurs, moving the O 2p level up and narrowing the direct

fundamental band gap. Therefore, the band-gap of the ZnO:Au is smaller than that of the ZnO. Different from the absorption spectra of undoped ZnO, the ZnO:Au has an obvious band-tail absorption, which is a reflection of defect density induced by incorporation of Au into ZnO.

In addition, a small absorption peak is observed at 2.0–2.4 eV in the absorption spectra of the ZnO:Au annealed at a temperature range of 600–800 °C, and its intensity increases with increasing annealing temperature. It is known from Table 1 that some $\text{Au}_{\text{Zn}}^{1+}$ escape from the ZnO:Au and form metal in the film as annealing temperatures of 600–800 °C. Based on literature reported previously [34], the small peak should be attribute to the local surface plasmon resonance (LSPR) absorption of Au deposited on ZnO. It is reported that the LSPR intensity increases with increasing the amount of Au/ZnO interface [35–37]. Therefore, the increase of the LSPR intensity is due to increase of the amount of Au^0 with increasing annealing temperature, since the more the content of Au^0 , the more the interface.

In order to investigate further the effect of Au doping on the optical properties of ZnO films, room temperature photoluminescence measurement was performed for the ZnO:Au and ZnO annealed at 600 and 800 °C. It is found that both annealed ZnO show strong PL emissions, one is an ultraviolet (UV) band originating from the near-band emission, and the other is a wide visible band originating from the defects emission, as shown in Fig. 6(a) and (b). However, the ZnO:Au film has no emission peak in the wavelength region from the UV to visible when annealed below 600 °C, as shown in Fig. 6(c), but show two very weak emission peaks as annealed at 800 °C compared to the ZnO that annealed at 800 °C, as shown in Fig. 5(d). This repeatable experimental phenomenon is obviously contrary to the literatures reported previously, where UV luminescence is enhanced for noble metal nanoparticle (Ag, Au)/ZnO nanocomposite [38,35,39]. It is noted from the reported literatures that Au is not incorporated into ZnO, but exists in the form of metal Au on the surface of ZnO in the noble metal/ZnO nanocomposite, which formed the metal-semiconductor contact and enhanced the electron transfer between Au and ZnO, resulting in the UV luminescence enhancement. With the combination analysis of the reported literatures and our experimental results, it is confirmed that the room temperature PL quenching of the ZnO:Au is attributed to the substitutional doping of Au in the ZnO films. It can be seen from the XPS calculation results that the relative content of $\text{Au}_{\text{Zn}}^{1+}$ significantly decreases from 3.5 at.% to 1.5 at.% as the annealing temperature increases from 350 °C to 800 °C. That is to say, only the 800 °C-annealed ZnO:Au with the smallest $\text{Au}_{\text{Zn}}^{1+}$ content has emission peaks, while both the band edge and visible emissions of the 350 and 600 °C-annealed samples with higher $\text{Au}_{\text{Zn}}^{1+}$ content are completely quenched. Hence, it is responsible to propose that the PL quenching is attribute to the existence of nonradiative recombination centers induced by $\text{Au}_{\text{Zn}}^{1+}$ or defects related to $\text{Au}_{\text{Zn}}^{1+}$ in the ZnO:Au film, moreover, the quenching degree is proportional to the content of $\text{Au}_{\text{Zn}}^{1+}$ in the films. We now take up the investigation of PL quenching in the ZnO:Au films, but do not understand well the transport and kinetic process of the quenching effect now. Therefore, the mechanism of PL quenching in the Au doped ZnO films will be studied in detail in our subsequent work.

4. Conclusions

The ZnO:Au films were prepared by radio frequency magnetron sputtering and post annealing techniques. It is found that the Au exists in the chemical state of $\text{Au}_{\text{Zn}}^{1+}$ in the as-grown ZnO:Au film, but begins to precipitate from the ZnO:Au and exists in the form of metal Au in the grain boundaries of the ZnO:Au as the ZnO:Au

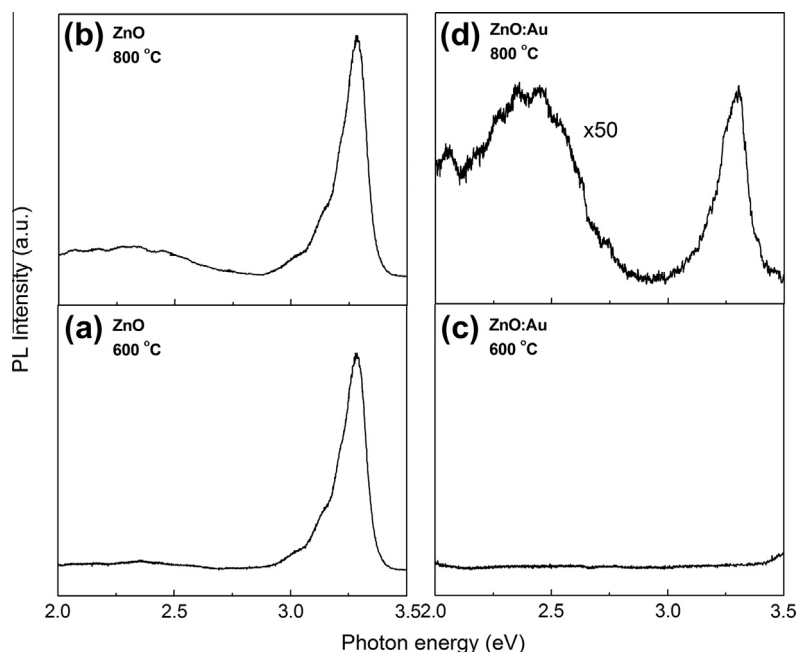


Fig. 6. Photoluminescence spectra of the undoped ZnO annealed at (a) 600 °C, (b) 800 °C and the ZnO:Au annealed at, (c) 600 °C, and (d) 800 °C.

is annealed at temperatures above 600 °C, implying that the solid solubility of Au in ZnO decreases with increasing temperature. The $\text{Au}_{\text{Zn}}^{1+}$ acts as acceptor, and p-type conductivity is observed in the 350 °C-annealed ZnO:Au, but the conductivity changes gradually from p-type to n-type with increasing annealing temperature due to decrease in the content of $\text{Au}_{\text{Zn}}^{1+}$. The optical band-gap of the ZnO:Au shows red-shift compared to ZnO, which is attributed to the shift up of O 2p level induced by strong p-d coupling between O and Au. The room temperature PL quenching occurs in the ZnO:Au annealed below 800 °C, which may be due to existence of nonradiative recombination center formed by the $\text{Au}_{\text{Zn}}^{1+}$ or the defects related to the $\text{Au}_{\text{Zn}}^{1+}$. The present work indicates that p-type ZnO can be obtained by Au doping, but it is still needed further optimize experimental method and technique to improve its electrical and luminescence properties.

Acknowledgements

This work was supported by the National Natural Science Foundation of China under Grant Nos. 10874178, 11074093, 61205038 and 11274135, Natural Science Foundation of Jilin province under Grant No. 201115013, and National Found for Fostering Talents of Basic Science under Grant No. J1103202.

References

- [1] D.C. Look, D.C. Reynolds, J.W. Hemsky, R.L. Jones, J.R. Sizelove, *Appl. Phys. Lett.* 75 (1999) 811.
- [2] S.H. Mohamed, *J. Alloys Comp.* 510 (2012) 119–124.
- [3] Jun Wang, Dongmei Li, Yaping Wang, *J. Alloys Comp.* 582 (2014) 1–5.
- [4] M.M. Rashad, E.M. Elsayed, M.S. Al-Kotb, A.E. Shalan, *J. Alloys Comp.* 581 (2013) 71–78.
- [5] Jianzi Li, Xu Jian, Xu Qingbo, Gang Fang, *J. Alloys Comp.* 542 (2012) 151–156.
- [6] Huiyun Xia, Taihong Liu, Lining Gao, Luke Yan, Wu Junwen, *Appl. Surf. Sci.* 258 (2011) 254–259.
- [7] H. Xiong, J.N. Dai, Xiong Hui, Y.Y. Fang, W. Tian, D.X. Fu, C.Q. Chen, Mingkai Li, Yunbin He, *J. Alloys Comp.* 554 (2013) 104–109.
- [8] Xiaozhu Li, Yongqian Wang, *J. Alloys Comp.* 19 (2011) 5765–5768.
- [9] D.C. Look, T.C. Droubay, S.A. Chambers, *Appl. Phys. Lett.* 101 (2013) 102101.
- [10] J. Smith, A.A. Sharbaf, M.J. Ward, M.W. Murphy, G. Fanchini, T.K. Sham, *J. Appl. Phys.* 113 (2013) 093104.
- [11] Danhui Zhang, Xiaoheng Liu, Xin Wang, *J. Alloys Comp.* 509 (2011) 4972–4977.
- [12] Audrius Alkauskas, Jhon L. Lyons, Daniel Steiauf, Chris G. Van de Walle, *Phys. Rev. Lett.* 109 (2012) 267401.
- [13] L.J. Mandalapu, Z. Yang, S. Chu, J.L. Liu, *Appl. Phys. Lett.* 92 (2008) 122101.
- [14] Y.F. Li, B. Yao, R. Deng, B.H. Li, J.Y. Zhang, Y.M. Zhao, *J. Phys. D: Appl. Phys.* 42 (2009) 105102.
- [15] B. Wang, L.D. Tang, J.G. Qi, H.L. Du, *J. Alloys Comp.* 503 (2010) 436–438.
- [16] S.S. Lin, *Appl. Phys. Lett.* 101 (2012) 122109.
- [17] L.Q. Zhang, Z.Z. Ye, J.Y. Huang, *J. Alloys Comp.* 509 (2011) 7405–7409.
- [18] D. Wang, J.W. Zhang, Y.P. Peng, Z. Bi, *J. Alloys Comp.* 478 (2009) 325–329.
- [19] J. Karamedel, C.F. Dee, K.G. Saw, B. Varghese, C.H. Sow, I. Ahmad, B.Y. Majlis, *J. Alloys Comp.* 512 (2012) 68–72.
- [20] C.K. To, B. Yang, S.C. Su, C.C. Ling, *J. Appl. Phys.* 110 (2011) 11352.
- [21] T. Yang, B. Yao, T.T. Zhao, G.Z. Xing, *J. Alloys Comp.* 509 (2011) 5426–5430.
- [22] J.G. Lu, Y.Z. Zhang, Z.Z. Ye, Y.J. Zeng, H.P. He, L.P. Zhu, J.Y. Huang, L. Wang, J. Yuan, B.H. Zhao, X.H. Li, *Appl. Phys. Lett.* 89 (2006) 112113.
- [23] M.A. Myers, M.T. Myers, M.J. General, J.H. Lee, L. Shao, H. Wang, *Appl. Phys. Lett.* 101 (2012) 112101.
- [24] Y. Yan, M.M. Al-Jassim, S.H. Wei, *Appl. Phys. Lett.* 89 (2006) 181912.
- [25] H.P. He, S.L. Li, L.W. Sun, Z.Z. Ye, *Phys. Chem. Chem. Phys.* 15 (2013) 7484–7487.
- [26] H.L. Pan, B. Yao, T. Yang, Y. Xu, *Appl. Phys. Lett.* 97 (2010) 142101.
- [27] H.S. Kang, B.D. Ahn, J.H. Kim, G.H. Kim, S.H. Lim, H.W. Chang, S.Y. Lee, *Appl. Phys. Lett.* 88 (2006) 202108.
- [28] X.D. Zhang, P. Wu, Y.Y. Shen, *Appl. Surf. Sci.* 258 (2011) 151–157.
- [29] D.W. Langer, C.J. Vesely, *Phys. Rev. B* 2 (1970) 12.
- [30] Eric Irissou, Marie-Chantal Denis, *Thin Solid Film* 472 (2005) 49–57.
- [31] N.M. Figueiredo, N.J.M. Carvalho, A. Cavaleiro, *Appl. Surf. Sci.* 257 (2011) 5793–5798.
- [32] G.Z. Xing, B. Yao, C.X. Cong, T. Yang, Y.P. Xie, B.H. Li, D.Z. Shen, *J. Alloys Comp.* 457 (2008) 36–41.
- [33] Y.F. Li, B. Yao, Y.M. Lu, Y.Q. Gai, C.X. Cong, Z.Z. Zhang, D.X. Zhao, J.Y. Zhang, B.H. Li, *J. Appl. Phys.* 104 (2008) 083516.
- [34] Kwang-Soon Ahn, Todd Deutsch, Yanfa Yan, *J. Appl. Phys.* 102 (2007) 023517.
- [35] K.W. Liu, Y.D. Tang, C.X. Cong, *Appl. Phys. Lett.* 94 (2009) 151102.
- [36] Myung-Ki Lee, Tae Geun Kim, Woong Kim, *J. Phys. Chem. C* 112 (2008) 10079–10082.
- [37] Peihong Cheng, Dongsheng Li, Xiaoqiang Li, *J. Appl. Phys.* 106 (2009) 063120.
- [38] B.J. Niu, L. Wu, W. Tang, X.T. Zhang, *Crys. Eng. Commun.* 13 (2011) 3678–3681.
- [39] KE Shan-Li, L. Wu, KAN Cai-Xia, MO Bo, *Acta Phys.-Chim. Sin.* 28 (2012) 1275–1290.